ACS APPLIED MATERIALS & INTERFACES

Research Article

www.acsami.org

Surface Modification of Poly(D,L-Lactic Acid) Scaffolds for Orthopedic Applications: A Biocompatible, Nondestructive Route via Diazonium Chemistry

Hesameddin Mahjoubi,[†] Joseph M. Kinsella,[‡,§] Monzur Murshed,[∥,⊥,#] and Marta Cerruti*[,†]

[†]Department of Materials Engineering, McGill University, Montreal, Quebec H3A 0C5, Canada

[‡]Department of Bioengineering, McGill University, Montreal, Quebec H3A 0C3, Canada

[§]Department of Biomedical Engineering, McGill University, Montreal, Quebec H3A OC5, Canada

[∥]Faculty of Dentistry, McGill University, Montreal, Quebec H3A 2B2, Canada

[⊥]Division of Experimental Medicine, Department of Medicine, McGill University, Montreal, Quebec H3G 1Y6, Canada

[#]Shriners Hospital for Children, Montreal, Quebec H3G 1A6, Canada

Supporting Information

ABSTRACT: Scaffolds made with synthetic polymers such as polyesters are commonly used in bone tissue engineering. However, their hydrophobicity and the lack of specific functionalities make their surface not ideal for cell adhesion and growth. Surface modification of these materials is thus crucial to enhance the scaffold's integration in the body. Different surface modification techniques have been developed to improve scaffold biocompatibility. Here we show that diazonium chemistry can be used to modify the outer and inner surfaces of three-dimensional poly(D,L-lactic acid) (PDLLA) scaffolds with phosphonate groups, using a simple two-step method. By changing reaction time and impregnation procedure, we were able to tune the concentration of phosphonate groups present on the scaffolds, without degrading the PDLLA matrix. To test the effectiveness of this modification, we immersed the scaffolds in simulated body fluid, and characterized them with scanning electron microscopy, X-ray photoelectron spectroscopy, Raman, and infrared spectroscopy. Our results showed that a layer of hydroxyapatite particles was formed on all scaffolds after 2 and 4 weeks of immersion; however, the precipitation was faster and in larger amounts on the phosphonate-modified than on the bare PDLLA scaffolds. Both osteogenic MC3T3-E1 and chondrogenic ATDC5 cell lines showed increased cell viability/metabolic activity when grown on a phosphonated PDLLA surface in comparison to a control PDLLA surface. Also, more calcium-containing minerals were deposited by cultures grown on phosphonated PDLLA, thus showing the pro-mineralization properties of the proposed modification. This work introduces diazonium chemistry as a simple and biocompatible technique to modify scaffold surfaces, allowing to covalently and homogeneously bind a number of functional groups without degrading the scaffold's polymeric matrix.

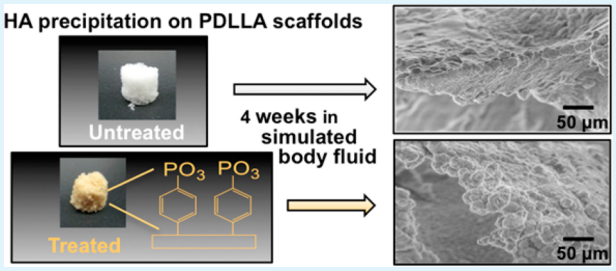

KEYWORDS: *scaffolds, surface modification, diazonium chemistry, biomineralization, PDLLA*

1. INTRODUCTION

Scaffolds are porous materials used in tissue engineering as platforms to enhance cell attachment, proliferation, and activity, leading to shorter healing time of injured or missing tissue.[1,2] Many natural and synthetic polymers are used to fabricate scaffolds;[3−5] among the synthetic ones, the most common ones are polyesters such as poly(D,L-lactic acid) (PDLLA) and poly(lactic-*co*-glycolic acid) (PLGA).[5−7] These polymers degrade by forming lactic acid and glycolic acid,[8,9] which are nontoxic. They are approved by the USA Food and Drug Administration for human clinical use.[10,11] Scaffolds made with polyesters are commonly used in bone tissue engineering[12,13] due to their biodegradability, biocompatibility, and adequate mechanical properties.[14]

The scaffold surface is the first region that cells get in contact with upon implantation, and determines their reaction to the implant.[15] Despite being biocompatible, polyesters are hydrophobic, which is a parameter known to promote nonspecific protein adsorption[16,17] and to prevent maximum adhesion and spreading of cells.[25,18] Moreover, they do not have any surface group that can specifically enhance cell adhesion, growth, or function.[7] Surface modification of these materials is thus crucial to enhance the scaffold's integration in the body.[6,7] When the scaffolds are used in orthopedic applications, surface modification can help the formation of hydroxyapatite

Received: September 3, 2013
Accepted: June 13, 2014
Published: June 26, 2014

   dx.doi.org/10.1021/am502752j | ACS Appl. Mater. Interfaces 2014, 6, 9975−9987

Table 1. Summary of Sample Name Abbreviations and Corresponding Preparation

sample name	form	duration of first step (amination)	duration of second step (phosphonation)	vacuum treatment?
PDLLA	scaffold	none	none	n/a
P-PDLLA-1h	scaffold	1 h	1 h	no
P-PDLLA-2h	scaffold	2 h	2 h	no
P-PDLLA-2h-VT	scaffold	2 h	2 h	yes
PDLLA-f	film	none	none	n/a
N-PDLLA-f	film	2 h	none	n/a
P-PDLLA-f	film	2 h	2 h	n/a

($Ca_{10}(PO_4)_6(OH)_2$) (HA), the mineral component of bones, a process known as biomineralization.[6,19] Plasma treatment was successfully applied to modify surfaces of bidimensional polymeric films,[20] but three-dimensional (3D) scaffolds cannot be easily functionalized with this technique because the plasma reacts quickly with the outer surfaces, while the inner pores do not get modified.[20] Scaffolds can be modified both on the outside and inside surfaces with two methods, physical adsorption or chemical modification.[21] With the first method, scaffolds are immersed in a solution containing biomolecules such as natural adhesive proteins.[22,23] This method has the advantage of simplicity, but leads to the formation of weak bonds, and the biomolecules can detach under physiological conditions.[24] To chemically modify a polyester scaffold, carboxylates and hydroxyl groups can be introduced via hydrolysis,[25,26] and biomolecules can then be bound to these groups.[27,28] However, the polymeric backbone of the scaffold is degraded during this treatment.[25,26]

Diazonium chemistry is a wet chemistry technique able to modify a variety of surfaces, including polymers,[29] carbon,[30] metals,[31] and oxides.[32] The grafting can be performed by applying an external potential[33] or exploiting redox reactions occurring between an aniline precursor,[34] which is transformed into a reactive radical, and the material to be modified. The method has been successful at introducing a number of functional groups, including alkyls, halides, carboxyls, nitro groups, perfluorinated chains, redox species, and dendrimers.[35] To the best of our knowledge, this technique has been used only once in the field of tissue engineering, to modify silk fibroin protein films.[36] In this work, several aniline derivatives were grafted on the surface of silk films to increase their hydrophilicity. Human mesenchymal stem cells easily attached, proliferated, and differentiated into osteogenic lineage on the modified films.[36] Still, up to now, no one has tested the effectiveness of diazonium chemistry on 3D scaffolds, or exploited its full potential to generate "self-adhesive surfaces".[34] One of the advantages of diazonium chemistry, in fact, is that the aniline layer formed can be easily reactivated and may react with any nucleophilic compound, thus allowing introducing almost any functional group on the desired surface.[37]

In this work, we show how diazonium chemistry can be used to modify PDLLA scaffolds homogeneously and nondestructively. Using a simple two-step procedure starting with a typical diazonium precursor, dianiline, we introduce phosphonate groups both on the outer and on the inner surfaces of the scaffolds, without degrading the polymeric backbone. We choose phosphonate groups because they are important components of noncollagenous proteins,[38,39] and are known to promote nucleation and growth of hydroxyapatite (HA) by attracting calcium cations.[40] Previous work showed that negatively charged groups such as carboxylic, hydroxyl, and phosphate groups are able to increase HA nucleation on PDLLA surfaces.[40] Our results show that upon immersion in simulated body fluid (SBF), HA precipitates faster and in larger amounts on phosphonate-modified PDLLA scaffolds than on bare PDLLA. In addition, we show that not only are the treated PDLLA surfaces cytocompatible but they are also able to improve the spreading and growth of MC3T3-E1 preosteoblast cells compared to unmodified PDLLA.

2. MATERIALS AND METHODS

2.1. Materials. PDLLA (number-average molecular weight, $\bar{M}_n$ = 110 000 g/mol) was a gift from Boehringer Ingelheim Canada. Sodium chloride (NaCl), *p*-phenylenediamine ($C_6H_4(NH_2)_2$), sodium nitrite ($NaNO_2$), hypophosphorous acid solution (50 wt % in H_2O) (H_3PO_2), 2-aminoethylphosphonic acid ($H_2NCH_2CH_2P(O)(OH)_2$) (AEPA), sodium hydrogen carbonate ($NaHCO_3$), potassium chloride (KCl), dipotassium hydrogen phosphate trihydrate ($K_2HPO_4{\cdot}3H_2O$), magnesium chloride hexahydrate ($MgCl_2{\cdot}6H_2O$), calcium chloride ($CaCl_2$), sodium sulfate (Na_2SO_4), tris-hydroxymethyl aminomethane ($NH_2C(CH_2OH)_3$) (Tris), hydrochloric acid (HCl), and control hydroxyapatite powder (HA) were purchased from Sigma-Aldrich.

2.2. Scaffold and Thin Film Preparation. Scaffolds were prepared using the solvent casting and particulate leaching method.[41] A 40% (w/w) PDLLA solution in acetone was prepared and mixed with sieved NaCl with particle sizes ranging from 150 to 350 μm. The mixture was then casted in a Pyrex Petri dish. The discs formed in the dish were left to dry in a vacuum at room temperature (RT) for 48 h. Cylindrical samples of 15 mm height and 9 mm diameter were extracted from the disc with cork borers of the same size by hand. The samples were then immersed in deionized (DI) water for 48 h, and the water was changed every 12 h to leach out the salt particles. The resulting porous scaffolds were then dried in vacuum at RT for 24 h.

To perform the cell culture experiments, PDLLA films (PDLLA-f, see Table 1) were prepared by pouring PDLLA polymer solution inside 35 mm diameter glass Petri dishes. The films were dried in vacuum at RT for 24 h, and a final thickness of 100 μm was achieved.

2.3. Surface Modification. *2.3.1. Scaffold Modification.* Scaffolds were modified with diazonium chemistry. A solution of 0.1 M aminophenyl diazonium cations ($NH_2{-}C_6H_4{-}N_2^+$) was prepared by dissolving 345 mg of $NaNO_2$ and 540 mg of *p*-phenylenediamine in 50 mL of 0.5 M HCl containing 17.85 mM H_3PO_2 (Scheme 3a–c). Two batches of ten PDLLA scaffolds were stirred in this solution for either 1 or 2 h to bind the diazonium cations to PDLLA, thus yielding amino-functionalized scaffolds. The samples were then rinsed and sonicated in DI water for 10 min to remove physisorbed diazonium cations. Amino-functionalized scaffolds were then immersed and stirred for either 1 or 2 h in a 10 mM solution of AEPA (Scheme 1), prepared in a 0.5 M solution of HCl containing also 5 mM $NaNO_2$

Scheme 1. Chemical Structure of 2-Aminoethylphosphonic Acid (AEPA)

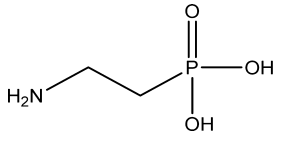

dx.doi.org/10.1021/am502752j | ACS Appl. Mater. Interfaces 2014, 6, 9975–9987

and 17.85 mM H_3PO_2. The samples were then rinsed and sonicated in DI water for 10 min and dried for 48 h in vacuum at RT. These samples were named "P-PDLLA-1h" and "P-PDLLA-2h" (see Table 1 for sample name abbreviations), where the letter "P" before PDLLA refers to the introduction of phosphonate groups on the scaffold surface.

To achieve a homogeneous modification on the outer and inner scaffold surfaces, a batch of eight scaffolds was treated in a different way, using a vacuum treatment. The reaction solution described above was frozen by liquid nitrogen in a vented Erlenmeyer flask, and the scaffolds and a magnetic stirrer were placed on top of the frozen solution. The flask was then connected to a vacuum to eliminate the air inside the scaffold pores, and then brought to RT. As the solution thawed, the scaffolds and the stir bar dropped in it, and the functionalization proceeded as explained above for the "P-PDLLA-2h" samples. These samples were named "P-PDLLA-2h-VT", where "VT" stands for "vacuum treatment" (Table 1).

2.3.2. Film Modification. Some of the PDLLA films prepared in 35 mm glass Petri dishes were left as such, and were used as control samples (PDLLA-f, see Table 1). Other films were further modified with diazonium chemistry, by immersing them for 2 h in 50 mL of 0.5 M HCl solution containing 345 mg of $NaNO_2$, 540 mg of *p*-phenylenediamine and 17.85 mM H_3PO_2. This led to a batch of amino-functionalized films (Scheme 3a–c, "N-PDLLA-f" samples, see Table 1). A second batch of samples was further treated following the same route used to introduce phosphonate groups on the scaffolds: the films were immersed for 2 h in a 10 mM solution of AEPA, prepared in a 0.5 M solution of HCl containing also 5 mM $NaNO_2$ and 17.85 mM H_3PO_2 (Scheme 3d). These samples are called "P-PDLLA-f" (see Table 1).

2.4. Immersion Tests. A batch of eight unmodified PDLLA scaffolds and one consisting of eight "2 h vacuum treated" samples were used for the immersion tests in simulated body fluid (SBF). The SBF solution was prepared according to Kokubo et al.,[42] and its composition is reported in Table 2. The scaffolds were immersed and stirred in SBF inside an incubator at 37 °C for 2 or 4 weeks. The SBF solution was changed every 3 days to better mimic the constant concentration present in body fluids.

Table 2. SBF Reagents and Their Concentration[42]

reagent	concentration (ppm)
NaCl	8035
$NaHCO_3$	355
KCl	225
$K_2HPO_4{\cdot}3H_2O$	231
$MgCl_2{\cdot}6H_2O$	311
$CaCl_2$	292
Na_2SO_4	72
Tris	6118

2.5. Characterization. Surface composition of the scaffolds was characterized by X-ray photoelectron spectroscopy (XPS) using a Thermo Scientific Kα spectrometer, equipped with an Al Kα X-ray source (1486.6 eV, 0.843 nm) and using an X-ray spot with a diameter of 400 μm. To prevent charging on the polymeric scaffolds, samples were hit with a flood gun shooting low energy electrons during the measurement. Scaffolds were cut using a Wilkinson razor blade and measurements were taken along the cross section of the samples. Spectral results were analyzed with the Thermo Avantage software (version 4.60).

Gel permeation chromatography (GPC) was conducted on a PDLLA sample and on both bare and surface modified PDLLA scaffolds, using a Waters Breeze chromatographer. The GPC was equipped with three Waters Styragel HR columns that were able to measure molecular weights in the range of 100–6 × 10^5 g mol^{-1}. All columns were operated at 40 °C and with a mobile phase flow rate of 0.3 mL min^{-1} during analysis. The GPC was equipped with both ultraviolet (UV 2487) and differential refractive index (RI 2410) detectors. The measurements were calibrated using poly(methyl methacrylate) standards dissolved in THF at 40 °C.

The surface morphology of the scaffolds after immersion in SBF was characterized using high resolution field emission scanning electron microscopy (FE-SEM, Hitachi high resolution field emission SU8000). The samples were analyzed without any coating and images were collected at an acceleration voltage of 0.5 kV.

Raman spectra of the scaffolds after immersion in SBF were recorded on a setup composed of a Bruker Senterra confocal Raman microscope connected to a Bruker MultiRAM stand-alone FT-Raman spectrometer. The 1032 nm laser of the MultiRAM was brought by a fiber optic cable through the Senterra microscope, and the spectra were acquired using a 40× objective, ranging from 0 to 3600 cm^{-1} with 256 scans at 3.5 cm^{-1} resolution. The collected signal was brought back to the MultiRAM detector via a second fiber optic cable.

To perform infrared (IR) spectroscopy, the particles precipitated on the scaffolds after immersion in SBF were extracted by dissolving the polymeric scaffold matrix in acetone, stirring for 2 h. The powders were separated from the polymeric solution by filtering and vacuum drying for 24 h. IR spectra of the extracted particles were collected on a Bruker Tensor 27 FT-IR spectrometer in diffuse reflectance (DRIFT) mode. The powders were diluted with an approximate 50% weight/weight ratio of KBr, and the spectra were collected from 400 to 4000 cm^{-1} using a DTGS detector, with 256 scans at 4 cm^{-1} resolution.

2.6. Cell Culture. Chondrogenic ATDC5 cells were received as a generous gift from Dr. Pierre Moffat, Shriners Hospital for Children, Canada, and Murine MC3T3-E1 preosteoblasts (subclone 14) were purchased from American Type Culture Collection (CRL-2594). Both the cell types were cultured in Minimum Essential Medium alpha containing 2 mM L-glutamine (MEM α, Gibco, Invitrogen) supplemented with 10% Fetal Bovine Serum (Hyclone, Canada) and 100 U/ml penicillin–streptomycin (Invitrogen, Canada) at 37 °C under 5% CO_2 in a humidified incubator. Prepared PDLLA, aminated and phosphonated films in 35 mm glass Petri dishes were sterilized by immersion in absolute ethanol for 10 min before seeding the cells. ATDC5 and MC3T3-E1 cells were seeded in triplicates on the films at densities of 2.0 × 10^6 and 5.0 × 10^6 cells/cm^2 for the proliferation and mineralization assays, respectively. To induce mineralization, cells were differentiated by adding ascorbic acid (100 μg/mL), β-glycerol phosphate (5 mM), and dexamethasone (10 mM) to the culture medium.

2.7. Alamar Blue and MTT Reduction Assays for Assessment of Cell Viability/Metabolic Activity. To examine cell viability/metabolic activity in each culture, Alamar Blue solution was directly added to the medium after 4 days of culture at a 100 μM final concentration. The reduction of Alamar Blue was measured fluorometrically (excitation at 560 nm and emission at 610 nm) using a microplate reader (Infinite 200, Tecan) after 1, 2, 3, and 4 h of incubation at 37 °C.

2.8. Evaluation of Cell Culture Mineralization by Alizarin Red Staining. For quantification of deposited minerals, ATDC5 and MC3T3-E1 cultures grown in the differentiation medium for 3 weeks were stained with 40 mM Alizarin Red solution (pH 4.0) for 5 min and thoroughly washed in deionized water. Images were taken at room temperature using a light microscope (DM200; Leica) with 10× objective. Images were captured using a digital camera (DP72; Olympus), acquired with DP2-BSW software (XV3.0; Olympus), and processed using PhotoShop (Adobe, San Jose, CA, USA). For quantification of the deposited minerals, bound dye was dissolved in 10% glacial acetic acid and measured spectrophotometrically at 405 nm using a microplate reader (Infinite 200, Tecan).

2.9. Statistical Analysis. All results are shown as standard deviation of the mean. Statistical analyses were performed by Student's *t*-test or one way ANOVA with $p < 0.05$ considered significant as indicated by a single asterisk.

3. RESULTS AND DISCUSSION

Surface modification of scaffolds for tissue engineering is crucial to improve their effectiveness and success once implanted. In this paper, we explore diazonium chemistry as a method to modify 3D PDLLA scaffolds homogeneously and non-destructively. With this technique, an aryldiazonium salt is dissolved in a weak acidic solution to generate aryldiazonium cations (Scheme 2).[34,43,44] These cations can be easily reduced to form stable radicals that are able to attack and bind to many different surfaces.[34,43,45]

Scheme 2. General Chemical Structure of an Aryldiazonium Cation[a]

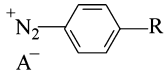

[a]R stands for a variety of functional groups, which can be organic or organometallic substituents, and A^- is the counteranion.

Scheme 3 shows the procedure that we used to modify the scaffolds. This is based on the method proposed by Viel et al.,[34] which uses a redox grafting strategy as opposed to the electrografting earlier proposed by Lyskawa et al.[44] In this method, the aryldiazonium cations are formed in situ through the reduction of *p*-phenylenediamine. In step a, one equiv of $NaNO_2$ was added to an acidic solution of *p*-phenylenediamine. This step leads to the predominant formation of the aminophenyl monosubstituted diazonium cations, $NH_2-C_6H_4-N_2^+$ shown in Scheme 3a; most likely, bisdiazonium cations are more difficult to form for electrostatic reasons and because the second amine left on the monodiazonium cation is less reactive toward diazotation.[44]

In step b, the aminophenyl diazonium cation was reduced to a stable aminophenyl radical ($NH_2-C_6H_4*$), using H_3PO_2 as a reducing agent. In the original method by Viel et al, Fe powder is used as a reducing agent instead of H_3PO_2. However, other work shows the anchoring of diazonium cations to a variety of nonreducing surfaces using H_3PO_2 as a reducing agent in place of Fe.[45,46] The mechanism by which H_3PO_2 is able to reduce aromatic diazonium cations to radicals is described in detail by Galli.[47] We chose H_3PO_2 instead of Fe because Fe powder would otherwise adhere to our scaffolds and be very hard to remove after the coupling. The reduction of aromatic diazonium cations leads to the formation of aminophenyl radicals ($NH_2-C_6H_4*$).[45] Aminodiazenyl radicals ($NH_2-C_6H_4-N_2*$, shown in Scheme 3b)[47] were speculated to be formed as well,[48] although this point is controversial.[49]

In step c, scaffolds were immersed in the solution containing the radicals formed by the reduction of diazonium cations, and a multilayer structure similar to that shown in Scheme 3c was formed on their surface.[34,48] Such a structure was called "polyaminophenylene" (PAP) layer by Viel et al.[34] and we will keep this terminology in this paper. The PAP layer contains azo (N=N) bridges, possibly because of the reaction with the aminodiazenyl radicals,[48] or via other more complex routes.[49]

Scheme 3. Functionalization of PDLLA scaffolds: (a) Aminophenyldiazonium Cation Generation from the *p*-Phenylenediamine in Solution; (b) Reduction of the Aminophenyldiazonium Cations with H_3PO_2; (c) Grafting of Aminophenyl and Azoaminophenyl Radicals onto Scaffold Surface and Formation of the PAP Layer; (d) Grafting of AEPA on the PAP Layer Formed on the Scaffold Surface[a]

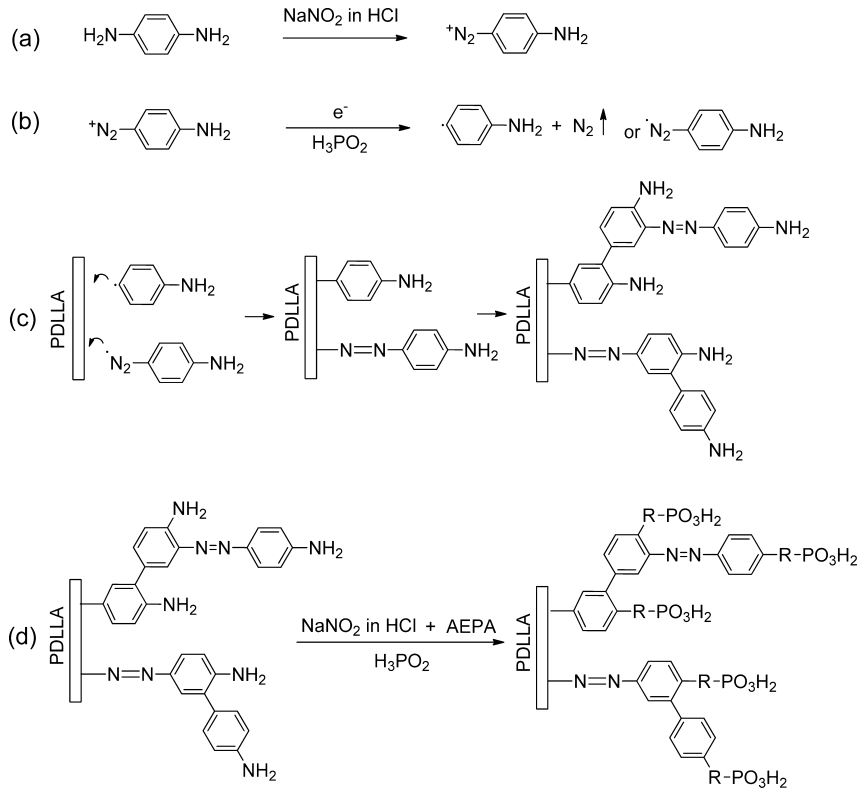

[a]R, shown at the end of step d, can stand for different structures, such as $-NH-CH_2-CH_2-$ (see the Supporting Information for more details).

In step d, the aminated scaffolds were washed and put in an acidic solution containing AEPA, $NaNO_2$, and H_3PO_2. $NaNO_2$ is added to diazotize the PAP layer, thus transforming it into a "polydiazophenylene" film (PDP).[34,48] The diazonium cations on the PDP layer are then reduced to radicals again by H_3PO_2. These radicals react with AEPA, resulting in the formation of a phosphonate-terminated multilayer with a structure similar to that shown in Scheme 3d. The exact product and the mechanism of this coupling reaction is not clear; however, its success and the presence of phosphonate terminal groups are proven by our XPS results (see below). When Viel et al. showed the coupling of PDP layers with amines, they did not discuss either the mechanism or the final products obtained on the surface.[34] The same can be said for other papers on coupling amine-containing biomolecules to PDP layers.[50−53] Additionally, generally, H_3PO_2 is not added in this second step, and the coupling is thought to occur because of the reaction between nucleophilic groups and the diazonium cations formed upon reduction of the PAP layer with $NaNO_2$.[34,51−53] However, triazenes should be formed by reaction between diazonium cations and primary amines,[54] and these compounds are highly unstable (see refs 54 and 55 and the Supporting Information). We have performed some experiments in the absence of H_3PO_2 and have shown that AEPA is not bound to the PDP layer in this case (see the Supporting Information). Thus, we believe that the coupling between AEPA and PDP proceeds via a radical mechanism, thanks to the addition of H_3PO_2. A thorough discussion of this hypothesized mechanism is provided in the Supporting Information; however, a detailed analysis of the coupling between PDP and primary amines will be the subject of a forthcoming paper.

Figure 1 shows a control PDLLA scaffold and a P-PDLLA-2h scaffold (see Table 1 for sample name abbreviations). The

Figure 1. (Left) photograph of an untreated PDLLA scaffold. (Right) photograph of a P-PDLLA-2h scaffold. The color change is due to presence of azo bridges (−N═N−) on the scaffold.

brownish color of the treated scaffold is due to the presence of azo bridges[56] (−N═N−). This visually shows the successful formation of the PAP layer shown in steps c and d in Scheme 3.

Table 3 shows the atomic composition of the inner and outer surfaces measured by XPS on the P-PDLLA-1h, P-PDLLA-2h, and P-PDLLA-2h-VT samples. Almost double amounts of N and P were measured on the outer surfaces of the 2 h treated samples compared with the 1 h treated samples. This increase indicated that the amount of functional groups introduced on the surface can be controlled by simply changing the reaction

Table 3. XPS Survey Data Measured on Surface Modified Scaffolds[a]

		relative elemental composition on the surface (atom %)		
sample	surfaces	N	P	Cl
P-PDLLA-1h	outer	1.6 ± 0.3	0.7 ± 0.2	
	inner			
P-PDLLA-2h	outer	3.4 ± 0.2	1.3 ± 0.1	0.1 ± 0.0
	inner	1.4 ± 0.2	0.3 ± 0.2	
P-PDLLA-2h-VT	outer	3.9 ± 0.1	1.1 ± 0.2	0.3 ± 0.1
	inner	2.5 ± 0.2	1 ± 0.1	0.2 ± 0.1

[a]See Table 1 for sample descriptions. All the data are averages of at least 10 values, ± the standard deviation.

time. The survey data measured along the cross section of both P-PDLLA-2h and P-PDLLA-1h showed that the functionalization was not homogeneous, and the inner core contained a much smaller amount of both N and P compared to the outer surfaces, which were in direct contact with the reaction solution. To solve this problem, we functionalized the samples under vacuum, to remove the air trapped in the scaffold pores and generate a driving force for the diazonium solution to penetrate throughout the core of the scaffold. This resulted in a much more homogeneous functionalization, involving the same amount of grafted AEPA on the outer and inner surfaces of the scaffolds, as can be seen by the almost identical P%. A higher amount of N was still visible on the outer surfaces of the scaffolds, possibly due to the fact that in step c (Scheme 3) the covalent bonding of the aryldiazonium cations was so fast that a larger number of them reacted with the scaffold surface despite the driving force created by the vacuum inside the scaffold pores. Some samples contained traces of chlorine, possibly because of not complete removal of HCl during the rinsing.

We can understand better the structure of the AEPA layer bound to the scaffolds by analyzing high resolution XPS spectra. Figure 2 shows the high resolution spectra for N_{1s}, P_{2p}, and C_{1s} before and after treatment via diazonium chemistry.

Although no N is present on the scaffolds before the treatment (Figure 2A), the N_{1s} spectrum for the P-PDLLA-2h-VT sample (Figure 2B) shows the presence of amino groups (peak at binding energy (BE) of 399.4 eV),[57] which was previously reported for films prepared by diazonium chemistry via reduction of aminophenyl groups.[58] This peak actually contains a component also related to azo bridges (−N═N−), normally found at 400 eV.[48,49,57] The presence of azo bridges has been previously reported on PDP layers, and its origin has been attributed either to the reaction of aminodiazenyl radicals,[48] or to the reaction between aryl radicals and diazonium cations.[49] The shoulder found at higher BE (401.9 eV) can be related to the presence of ammonium groups ($-NH_3^+$).[30,59] The formation of ammonium groups explains the presence of chlorine found in the XPS survey spectra of some of the treated scaffolds as shown in Table 3, because chlorine can act as counterion for the positively charged ammonium groups. The peak positioned at higher BE (406 eV) indicates the presence of nitro groups,[30,35,60] but the reason for the formation of these species is unclear. It is possible that they may form upon reaction with impurities,[30,35] or they may relate to the use of $NaNO_2$ in the coupling.[60]

Although no P was present on the untreated samples (Figure 2C), the P_{2p} spectra measured on the treated samples (Figure 2D) showed a peak centered at 134.1 eV, which corresponds

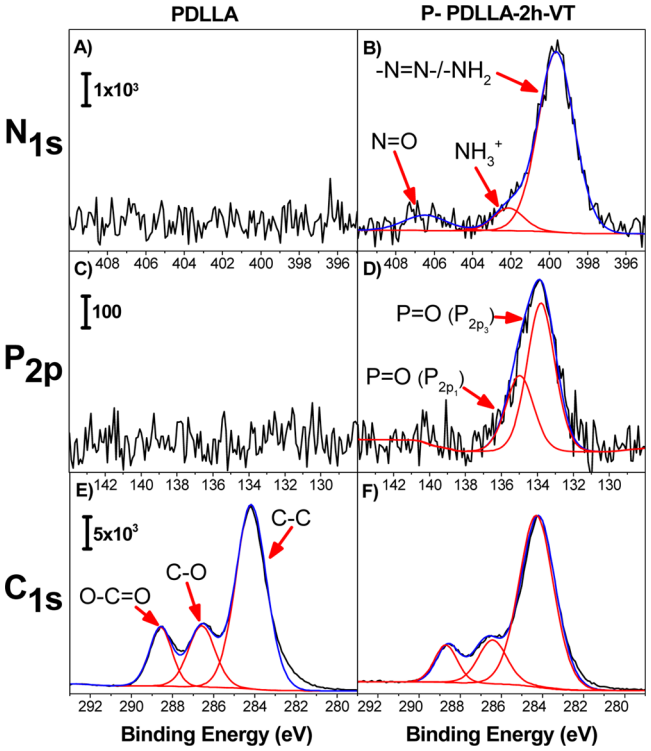

Figure 2. XPS high resolution spectra measured for N_{1s} (first row), P_{2p} (second row), and C_{1s} (third row) on unmodified PDLLA scaffolds (A, C, E), and P-PDLLA-2h-VT scaffolds (B, D, F). Experimental data are shown in black, peak fits in red, and the overall fit in blue.

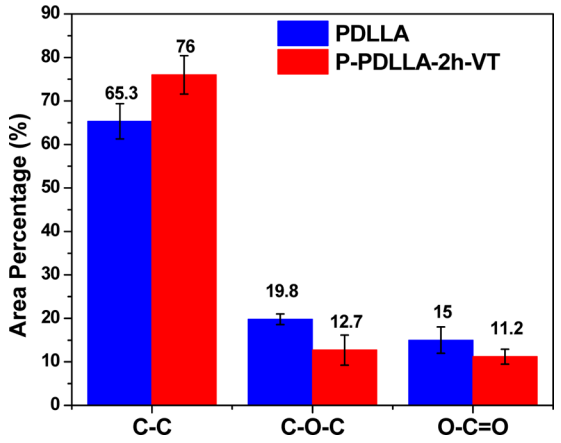

Figure 3. Relative amounts of different carbon species found on scaffolds before (PDLLA samples, blue) and after treatment (P-PDLLA-2h-VT samples, red), measured by integrating the areas of the three components present in C_{1s} high resolution XPS spectra at 284.4, 286.6, and 288.6 eV, respectively. All the data are averages of at least 10 values, ± the standard deviation.

Table 4. $\bar{M}_n$ and PDI Obtained by GPC for PDLLA, Untreated PDLLA Scaffolds, and P-PDLLA-2h-VT Scaffolds

	PDLLA polymer	PDLLA scaffold	P-PDLLA-2h-VT scaffold
$\bar{M}_n$ (g/mol)	202 645	195 718	200 280
PDI	1.82	1.69	1.74

well to a phosphonate group.[57] Previous researchers have reported P_{2p} peaks with BE ranging from 132.4 to 135.8 eV for titanium[61,62] and tantalum oxide[63] surfaces modified with phosphonic acid for biomedical applications.

Three components can be clearly distinguished on the C_{1s} spectra of PDLLA scaffolds both before and after treatment (Figure 2E,F), which can be related to C—C, C—O—C, and O═C—O bonds, with BEs of approximately 284.4, 286.6, and 288.6 eV, respectively.[57] Although the position of these components does not change significantly before and after treatment, their relative amount does (Figure 3). The increase in the relative amount of C—C bonds with respect to C—O—C and C═O bonds observed after treatment confirms the formation of the PAP layer and the coupling of AEPA on the surface of the scaffolds, because neither the PAP layer nor AEPA contain any carboxyl or carbonyl groups.

The XPS results confirmed that AEPA was successfully bound to PDLLA scaffolds via diazonium chemistry. The amount of bound molecules could be controlled by changing the reaction time, and a homogeneous modification was achieved using vacuum impregnation.

To be sure that the acidic conditions used during the diazonium treatment did not cause degradation of the PDLLA structure, we analyzed the samples by GPC. As shown in Table 4, $\bar{M}_n$ and polydispersity index (PDI) measured on a sample of PDLLA, an untreated PDLLA scaffold, and a P-PDLLA-2h-VT scaffold are approximately the same. This shows that the acidic conditions of the reaction solution did not cause degradation and changes in the polymer structure. Some changes in surface morphology occurred after the treatment, as shown in Figure 4. Although the untreated scaffolds present a smooth surface (Figure 4A), the P-PDLLA-2h-VT samples show a rougher surface (Figure 4B). This is to be related to the formation of the PAP layer (Scheme 3c), as previously observed when a similar procedure was used to functionalize smooth surfaces like graphite.[30] However, no signs of surface degradation such as formation of larger pores was observed, contrary to what previously found when PDLLA scaffolds were treated by hydrolysis.[25]

After proving that we could homogeneously modify the scaffolds without degrading their polymeric structure, we immersed them in SBF for up to 4 weeks. The goal of this experiment was to check if the phosphonate groups introduced were able to enhance HA precipitation on the scaffolds.

Figure 5 shows SEM images of the unmodified and P-PDLLA-2h-VT scaffolds after 2 and 4 weeks of immersion in SBF. Although no particles were observed before SBF immersion on both treated and untreated scaffolds (Figure 4), after 2 weeks of immersion, agglomerated particles obviously appeared on the surface of both types of scaffolds (Figure 5A,B). The treated samples were covered more homogeneously than the untreated ones, which still showed areas free from agglomerates. The agglomerates observed on the treated samples were bigger than those formed on the untreated ones. After 4 weeks of immersion (Figure 5C,D), the agglomerates increased in size for both the unmodified and the treated scaffolds; however, again, larger and more abundant agglomerates were observed on the treated samples. A high magnification image of the particles formed on the treated scaffolds immersed in SBF for 2 weeks is shown in Figure 6. A similar morphology was observed on all other samples, showing spherulitic particles composed by thin platelets. This morphology is typically observed for HA precipitation from solutions with Ca and P concentration close to plasma.[64]

dx.doi.org/10.1021/am502752j | ACS Appl. Mater. Interfaces 2014, 6, 9975−9987

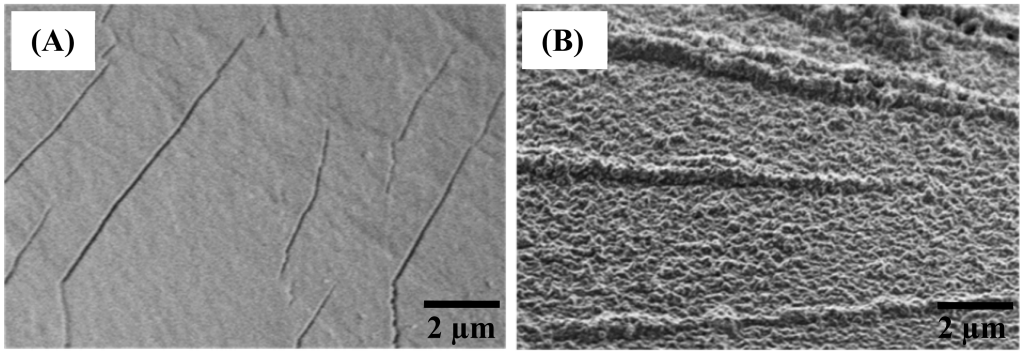

Figure 4. SEM images of the surface of (A) untreated scaffolds (B) P-PDLLA-2h-VT scaffolds.

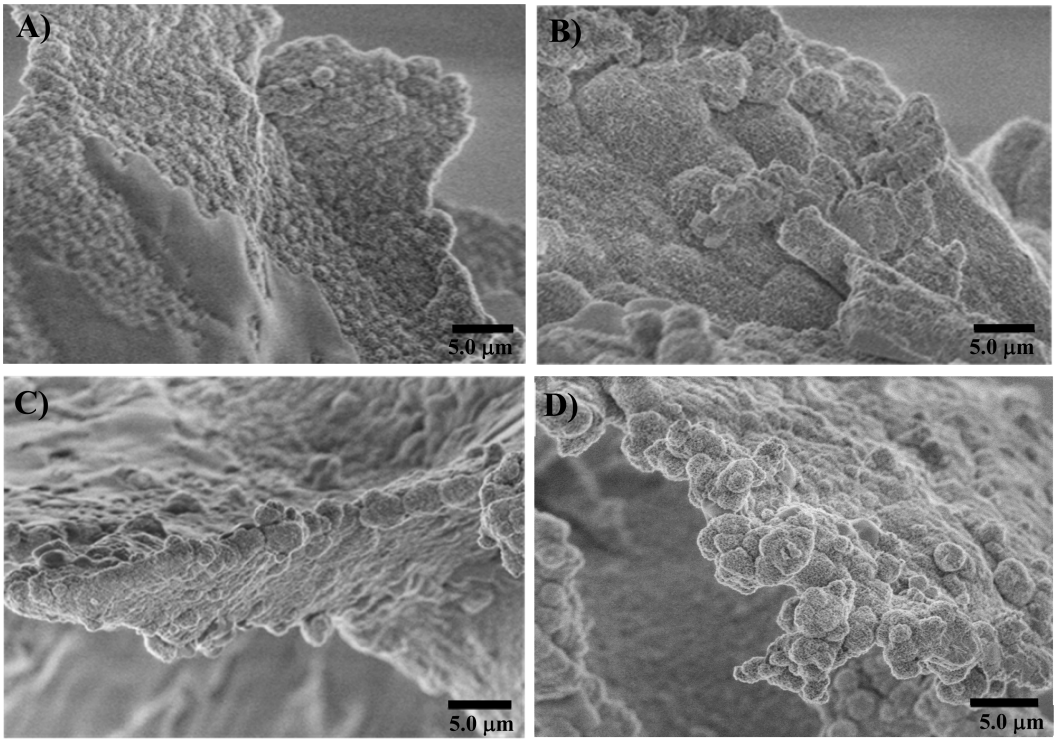

Figure 5. SEM images of untreated (A, C) and P-PDLLA-2h-VT (B, D) scaffolds immersed in SBF for 2 (A, B) and 4 (C, D) weeks.

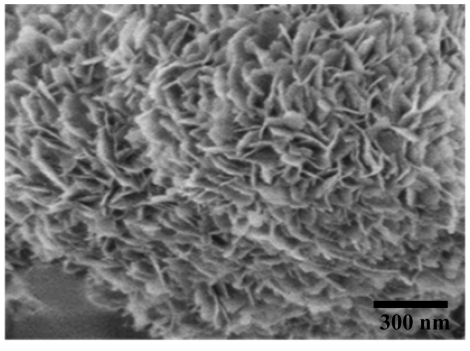

Figure 6. High magnification SEM image of the agglomerates present on the surface of P-PDLLA-2h-VT scaffolds after 2 weeks of immersion in SBF.

We performed XPS to obtain a more quantitative evaluation of the amount of precipitates formed on the scaffolds, as well as to understand their composition. XPS survey spectra showed the presence of Ca and P on the scaffold surfaces after SBF immersion (Figure 7). The Ca/P ratio measured on the precipitates found both on the inner and on the outer surfaces of the untreated scaffolds after both 2 and 4 weeks immersion was 1.6 ± 0.2, whereas for the treated scaffolds was 1.7 ± 0.2, which suggests that HA was formed on all samples. We observed larger amounts of both Ca and P outside than inside the scaffolds (Figure 7), probably because the HA particles deposited on the outer surface prevented the diffusion of Ca^{2+} and PO_4^{3-} ions inside the scaffolds. This suggests that most of the HA nucleation and growth occurred on the areas of the scaffolds more directly exposed to SBF. Higher amounts of both Ca and P were found on the treated than on the untreated samples, both on the outer and inner surfaces of the scaffolds, both at 2 and at 4 weeks immersion. This confirms the qualitative SEM observations, and suggests that the modification with phosphonate groups caused a larger number of Ca^{2+} cations to be attracted toward the scaffold surfaces, thus increasing the number of HA nucleation sites and the overall amount of HA particles deposited on the scaffolds.

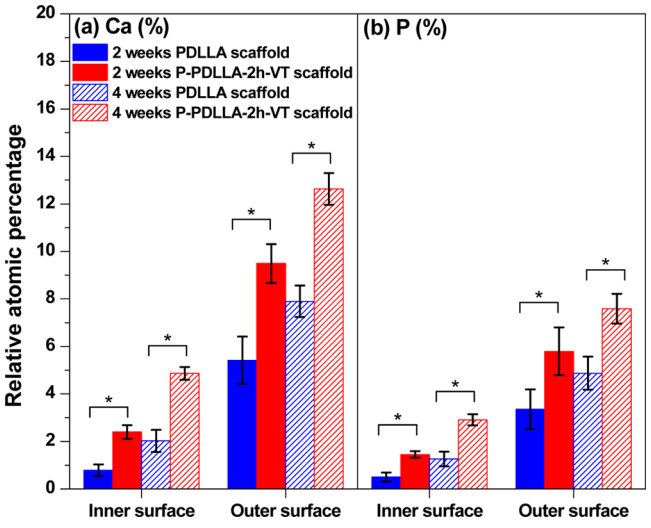

Figure 7. Relative atomic % of (a) Ca and (b) P on inner and outer surfaces of untreated (PDLLA, blue) and treated (P-PDLLA-2h-VT, red) samples immersed in SBF for 2 (solid filling) and 4 (striped filling) weeks. All the data are averages of at least 10 values, ± the standard deviation.

To confirm that the particles were indeed HA, we performed both Raman and IR spectroscopy on the samples. Figure 8

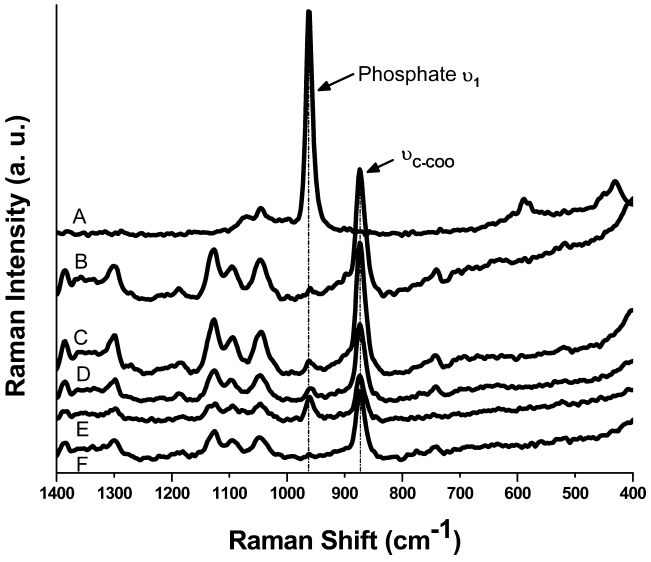

Figure 8. Raman spectra of untreated scaffolds after 2 and 4 weeks immersion in SBF (B and D, respectively) and P-PDLLA-2h-VT scaffolds after 2 and 4 weeks immersion in SBF (C and E, respectively) in comparison with control PDLLA scaffold (F) and HA (A). The areas under the bands marked with arrows are used for the quantitative analysis shown in Table 5.

shows the spectra collected on unmodified and P-PDLLA-2h-VT scaffolds immersed in SBF for 2 and 4 weeks, along with spectra collected on HA powders and on an untreated PDLLA scaffold. The four phosphate bands ν_1 (964 cm^{-1}), ν_2 (430 cm^{-1}), ν_3 (1046 cm^{-1}), and ν_4 (589 cm^{-1}) are clearly visible on the HA spectrum. Most of the peaks observed on the spectra relative to the scaffolds immersed in SBF relate to the PDLLA matrix, as can be seen by comparing them with the PDLLA spectrum. This is due to the fact that Raman is less surface sensitive than XPS (an approximately 1 μm thick surface layer is analyzed by Raman, and 3−10 nm by XPS), and thus more of the sample substrate is picked up by Raman than by XPS. Despite this, the ν_1 phosphate peak at 964 cm^{-1} is clearly visible on the spectra of all the immersed samples, and absent on that of the PDLLA control scaffold. To give some quantitative assessment based on these data, we calculated the ratio of the areas measured under the ν_1 phosphate peak and the ν_{C-COO} peak at 873 cm^{-1}[65] for each spectrum (Table 5). A much

Table 5. Ratio of the Areas Measured on the Raman Spectra under the Phosphate ν_1 Peak and the ν_{C-COO} Peak for Untreated and P-PDLLA-2h-VT Scaffolds after Immersion in SBF for 2 and 4 Weeks

	untreated		P-PDLLA-2h-VT	
	2 weeks	4 weeks	2 weeks	4 weeks
ν_1 (963 cm^{-1})/ C−COO(873 cm^{-1})	0.089	0.168	0.125	0.241

higher ratio was measured on the treated than on the untreated scaffolds both after 2 and 4 weeks of immersion in SBF, thus confirming that a higher amount of HA was formed on the treated samples.

To better understand the structure of the HA particles and their interaction with PDLLA, we collected IR spectra on the particles extracted from the scaffolds.

Figure 9 shows the FT-IR spectra of the extracted powders from untreated and P-PDLLA-2h-VT scaffolds after 2 and 4

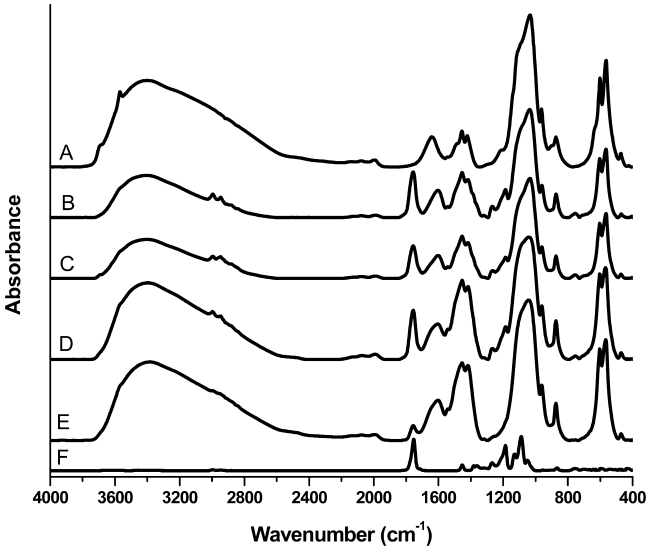

Figure 9. FT-IR spectra of powders extracted from untreated (B and D) and P-PDLLA-2h-VT (C and E) scaffolds after 2 (B and C) and 4 (D and E) weeks of immersion in SBF. The spectra of a PDLLA scaffold (F) and HA (A) are shown too.

weeks of SBF immersion, along with the spectra of a PDLLA scaffold and of HA. All samples show the same peaks that are present in the spectrum of HA, and a few bands related to the polymer. The assignments of the peaks found on the spectra of the scaffolds after immersion in SBF related to HA and PDLLA are shown in Tables 6 and 7, respectively. The IR bands related to HA are present in the spectra of all the scaffolds and are in good agreement with data reported by Rehman et al.[66] for several commercial HA powders. The only band that is present in the control HA powder but not on the powders extracted

dx.doi.org/10.1021/am502752j | ACS Appl. Mater. Interfaces 2014, 6, 9975−9987

Table 6. Assignments of the IR Bands Relative to HA, Found on HA Control and on the Powders Extracted from Untreated and P-PDLLA-2h-VT Scaffolds after Immersion in SBF for 2 and 4 Weeks[a]

		2 weeks immersion in SBF		4 weeks immersion in SBF	
peaks (cm^{-1})	HA control	PDLLA	P-PDLLA-2h-VT	PDLLA	P-PDLLA-2h-VT
hydroxyl stretch	3568				
carbonate ν_3					
-(m)	1643	1602	1602	1602	1602
-(m)	1455	1452	1452	1452	1452
-(m)	1422	1423	1423	1422	1422
phosphate ν_3					
-(sh)	1092	1088	1090	1087	1087
-(vs)	1034	1035	1035	1041	1041
phosphate ν_1	962	961	961	960	960
carbonate ν_2	875	873	873	874	874
phosphate ν_4					
-(s)	601	603	603	602	602
-(s)	564	565	565	567	566
phosphate ν_2 (w)	472	469	471	470	470

[a]See Figure 9.

Table 7. Assignments of the IR Bands Relative to PDLLA, Found on PDLLA Scaffold before Immersion and on the Powders Extracted from Untreated and P-PDLLA-2h-VT Scaffolds after Immersion in SBF for 2 and 4 Weeks[a]

	before immersion	2 weeks immersion in SBF		4 weeks immersion in SBF	
peaks (cm^{-1})	PDLLA scaffold	PDLLA	P-PDLLA-2h-VT	PDLLA	P-PDLLA-2h-VT
ν_{as} CH_3	2995 (m)	2995 (m)	2995 (m)	2995 (m)	2995 (m)
ν_s CH_3	2946 (m)	2946 (m)	2946 (m)	2945 (m)	2946 (m)
ν (C═O)	1753 (vs)	1756 (vs)	1756 (vs)	1756 (vs)	1754 (vs)
δ_{as} CH_3	1452				
δ_s CH_3	1382				
δ_i CH+ δ_s CH_3	1363				
δ CH+ ν COC	1269	1269	1269	1269	1269
ν_{as} COC	1186 (vs)				
r_{as} CH_3	1130 (s)				
ν_s COC	1088 (vs)				
ν C—CH_3	1049				
R CH_3+ νCC	957 (w)				
νCC—COO	867 (s)				
ν COO	754 (w)				

[a]See Figure 9.

from the scaffolds is the one at approximately 3570 cm^{-1}, related to the structural isolated OH groups in HA.[66] This absence may indicate a less ordered structured in the HA particles extracted from the scaffolds compared to the control HA. Also, all HA particles are carbonated as seen by the bands at around 1650 cm^{-1} and the one at 870 cm^{-1}, more intense in the particles extracted from our samples than in the HA control. The weak bands observed on the spectra of the particles extracted from the scaffolds at 2995 and 2946 cm^{-1} and the stronger ones at 1756 and 1269 cm^{-1} are related to the $\nu_{-CH3(asym)}$ and $\nu_{-CH3(sym)}$, and $\nu_{C=O}$ and ν_{C-O}, respectively (Table 7).[67,68] The presence of these bands indicates that some of the PDLLA from the scaffold matrix remained bound to the HA particles after their extraction. In fact, similar bands can be observed on the spectrum measured on pure PDLLA. The rest of the bands related to PDLLA fall in the same spectral region as the main peaks of HA, and thus cannot be observed. The presence of PDLLA peaks in the spectra of the extracted HA powders even after thorough acetone washes is remarkable, and suggests a strong (maybe covalent) interaction between the polymeric matrix and the HA particles nucleated on it.

To check the biocompatibility of the diazonium chemistry approach, we prepared bidimensional films treated in the same way as the three-dimensional scaffolds and examined the metabolic activities of chondrogenic ATDC5 and osteogenic MC3T3-E1 cells cultured on these films. We tested three types of films: PDLLA films (PDLLA-f), films modified only with the first step of the diazonium treatment (Scheme 3c, N-PDLLA-f), and other films modified with all the steps (Scheme 3d, P-PDLLA-f).

Figure 10 shows metabolic activities of 4-day-old ATDC5 and MC3T3-E1 cultures as indicated by their ability of reduce Alamar Blue dye after 1, 2, 3, and 4 h incubation at 37 °C. The constant increase of Alamar blue reduction by the cells over a period of 4 h shows that the cells are viable in all conditions. Although cells grown on N-PDLLA-f show lower Alamar Blue reduction compared to the control PDLLA-f, cells grown on the surface of P-PDLLA-f consistently show higher Alamar Blue reduction than control PDLLA-f over all time periods. This shows that the introduction of phosphonate groups by diazonium chemistry enhanced the total cell metabolic activity, which can be caused by increased cell viability and/or proliferation

The in vitro mineralization ability of cultured osteogenic or chondrogenic cell lines is often used as a determinant of their functional properties. To investigate the effects of surface modification on the mineral deposition properties of ATDC5 and MC3T3-E1 cells, we grew them in the presence of a differentiation medium (culture medium supplemented by ascorbic acid, β-glycerol phosphate, and dexamethasone) for 3 weeks. At the end of this period, we stained the cultures by Alizarin Red, a calcium binding dye. Figure 11a shows that all the cultures grown on the surface of PDLLA-f, N-PDLLA-f, and P-PDLLA-f deposited calcium-containing minerals. ATDC5 cells deposit more minerals than MC3T3-E1, which is to be related to intrinsic differences in mineral deposition properties between these two cell lines. The amount of bound Alizarin Red is quantified in Figure11b. For both ATDC5 and MC3T3-E1 cultures, P-PDLLA-f films show the highest amount of mineral deposition among the three surfaces analyzed. This data is complementary to the observed increase in metabolic activities in the cultures grown on P-PDLLA-f and suggests that the phosphonate groups introduced via diazonium treatment enhanced the pro-mineralization properties of PDLLA.

4. CONCLUSIONS

Diazonium chemistry is a simple method that can be used to modify a variety of surfaces with different functional groups. Here we have shown that 3D PDLLA scaffolds can be easily and effectively modified with diazonium chemistry without degrading their polymeric structure. By adopting a vacuum impregnation technique, we were able to modify both the inner

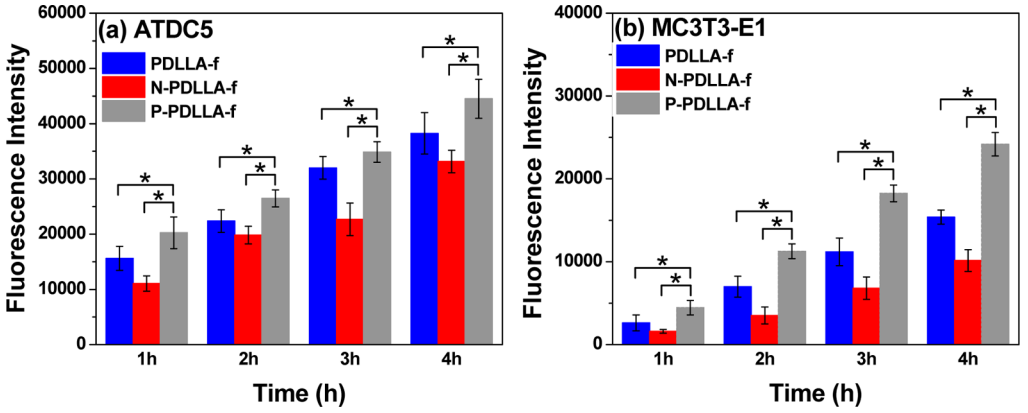

Figure 10. Alamar Blue assay of (a) ATDC5 chondrogenic cells and (b) MC3T3-E1 preosteoblasts seeded on PDLLA-f, N-PDLLA-f, and P-PDLLA-f films at a density of 2.0 × 106 cells/cm^2. The reduction of Alamar Blue was measured fluorometrically after 1, 2, 3, and 4 h of incubation at 37 °C (each sample was measured in triplicates at 560 nm excitation and 610 nm emission).

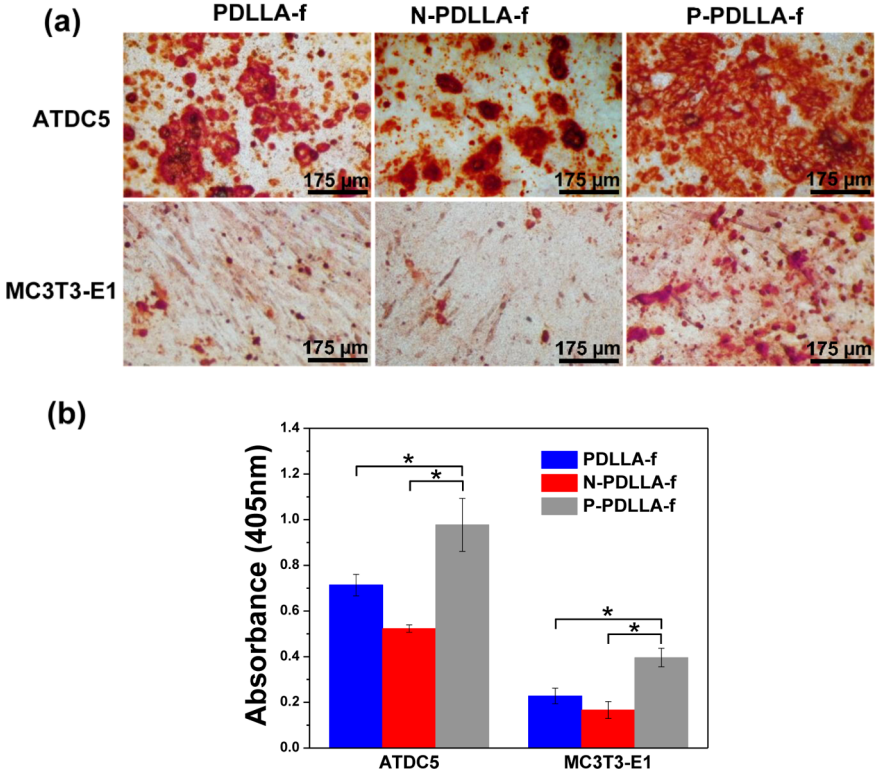

Figure 11. (a) Alizarin Red staining, (b) Absorbance of alizarin dye at 405 nm for ATDC5 and MC3T3-E1 preosteoblasts seeded on PDLLA-f, N-PDLLA-f, and P-PDLLA-f at a density of 5.0 × 106 cells/cm^2.

and the outer surfaces of the scaffolds homogeneously, and to tune the number of surface groups introduced by varying the functionalization time. After binding aryldiazonium cations on the scaffold surface, we successfully attached AEPA, and showed that phosphonate groups enhanced nucleation and growth of HA particles on the surfaces of PDLLA scaffolds after immersion in SBF. This surface modification could be used on scaffolds for orthopedic applications, because HA particles have excellent osteoconductivity and resorbability, and enhance bone growth and healing.[69]

In vitro experiments showed that the diazonium treatment is biocompatible: both chondrogenic ATDC5 and osteogenic MC3T3-E1 cell types were viable on PDLLA surfaces both treated with the first step of the treatment (aminated) and after the subsequent modifications (phosphonated). Cells cultured on phosphonated PDLLA films showed higher metabolic activity and deposited more calcium-containing minerals than those cultured on bare PDLLA. Given this positive result and the fact that phosphonate groups are known to inhibit bone resorption,[70] we suggest that phosphonate-functionalized scaffolds could be directly implanted, without necessarily preseeding them with HA.

The simplicity of this method, its biocompatibility, and the fact that PDLLA is not degraded during the treatment makes it an ideal candidate to modify scaffolds for a variety of biomedical applications. In fact, after producing a "self-adhesive" layer rich in amino groups, many other groups can be easily bound to the scaffold, of which phosphonates represent just an example. One could use a similar method to bind peptides or proteins eliciting specific cellular functions, to

dx.doi.org/10.1021/am502752j | ACS Appl. Mater. Interfaces 2014, 6, 9975−9987

make the scaffolds truly interactive with the surrounding tissues.

■ ASSOCIATED CONTENT

Supporting Information

Explanation in detail of the necessity of both $NaNO_2$ and H_3PO_2 to achieve the binding of AEPA to the PAP layer formed on PDLLA and the hypothesized mechanism of binding of AEPA to the PAP layer. This material is available free of charge via the Internet at http://pubs.acs.org.

■ AUTHOR INFORMATION

Corresponding Author

*Marta Cerruti, Ph.D. Address: Materials Engineering, McGill University, 3610 University St., 2M020 Wong Building, Montreal, QC H3A 0C5, Canada. E-mail: marta.cerruti@mcgill.ca. Phone: 1 (514) 398-5496. Fax: 1 (514) 398-4492.

Notes

The authors declare no competing financial interest.

■ ACKNOWLEDGMENTS

We acknowledge financial support from the Natural Sciences and Engineering Research Council of Canada (NSERC) "Discovery" program, the "Nouveaux chercheurs" program from Fonds de recherche du Québec - Nature et technologies (FQRNT), and the Canada Research Chair program. We thank Prof. Raynald Gauvin for allowing access to the FE-SEM and Dr. Nicolas Brodusch for collecting the images, Prof. Milan Maric for access to the GPC and Ms. Chi Zhang for help with the measurements, and Boehringer Ingelheim Canada for providing PDLLA. We also thank Dr. Xuan Tuan Le for fruitful discussions about diazonium chemistry, and Dr. Naser Muja for helpful suggestions on the cell culture work.

■ REFERENCES

(1) Hutmacher, D. W. Scaffolds in Tissue Engineering Bone and Cartilage. *Biomaterials* **2000**, *21*, 2529−2543.

(2) Freed, L. E.; Engelmayr, G. C.; Borenstein, J. T.; Moutos, F. T.; Guilak, F. Advanced Material Strategies for Tissue Engineering Scaffolds. *Adv. Mater.* **2009**, *21*, 3410−3418.

(3) Dhandayuthapani, B.; Yoshida, Y.; Maekawa, T.; Kumar, D. S. Polymeric Scaffolds in Tissue Engineering Application: A Review. *Int. J. Polym. Sci.* **2011**, *2011*, 1−19.

(4) Cheung, H.-Y.; Lau, K.-T.; Lu, T.-P.; Hui, D. A Critical Review on Polymer-Based Bio-Engineered Materials for Scaffold Development. *Composites, Part B* **2007**, *38*, 291−300.

(5) Liu, X. H.; Holzwarth, J. M.; Ma, P. X. Functionalized Synthetic Biodegradable Polymer Scaffolds for Tissue Engineering. *Macromol. Biosci.* **2012**, *12*, 911−919.

(6) Mahjoubi, H.; Abdollahi, S.; Cerruti, M. Surface Functionalization of Polymeric Scaffolds for Orthopedic Applications. In *Thin Films and Coatings in Biology*; Nazarpour, S., Chaker, M., Eds.; Biological and Medical Physics, Biomedical Engineering Series; Springer Publishing: Dordrecht, The Netherlands, 2013; Chapter 7.

(7) Jiao, Y. P.; Cui, F. Z. Surface Modification of Polyester Biomaterials for Tissue Engineering. *Biomed. Mater. (Bristol, U. K.)* **2007**, *2*, R24−37.

(8) Danmark, S.; Finne-Wistrand, A.; Schander, K.; Hakkarainen, M.; Arvidson, K.; Mustafa, K.; Albertsson, A. C. In Vitro and in Vivo Degradation Profile of Aliphatic Polyesters Subjected to Electron Beam Sterilization. *Acta Biomater.* **2011**, *7*, 2035−2046.

(9) Pamula, E.; Dobrzynski, P.; Bero, M.; Paluszkiewicz, C. Hydrolytic Degradation of Porous Scaffolds for Tissue Engineering from Terpolymer of L-Lactide, Epsilon-Caprolactone and Glycolide. *J. Mol. Struct.* **2005**, *744*, 557−562.

(10) Wu, X. S. Synthesis, Characterization, Biodegradation, and Drug Delivery Application of Biodegradable Lactic/Glycolic Acid Polymers: Part Iii. Drug Delivery Application. *Artif. Cells, Blood Substitutes, Biotechnol.* **2004**, *32*, 575−591.

(11) Jalil, R.; Nixon, J. R. Biodegradable Poly(Lactic Acid) and Poly(Lactide-co-Glycolide) Microcapsules: Problems Associated with Preparative Techniques and Release Properties. *J. Microencapsulation* **1990**, *7*, 297−325.

(12) Mano, J. F.; Sousa, R. A.; Boesel, L. F.; Neves, N. M.; Reis, R. L. Bioinert, Biodegradable and Injectable Polymeric Matrix Composites for Hard Tissue Replacement: State of the Art and Recent Developments. *Compos. Sci. Technol.* **2004**, *64*, 789−817.

(13) Zhang, X.; Hua, H.; Shen, X.; Yang, Q. In Vitro Degradation and Biocompatibility of Poly(L-Lactic Acid)/Chitosan Fiber Composites. *Polymer* **2007**, *48*, 1005−1011.

(14) Yang, S. F.; Leong, K. F.; Du, Z. H.; Chua, C. K. The Design of Scaffolds for Use in Tissue Engineering. Part 1. Traditional Factors. *Tissue Eng.* **2001**, *7*, 679−689.

(15) Chan, B. P.; Leong, K. W. Scaffolding in Tissue Engineering: General Approaches and Tissue-Specific Considerations. *Eur. Spine J.* **2008**, *17*, 467−479.

(16) Neff, J. A.; Caldwell, K. D.; Tresco, P. A. A Novel Method for Surface Modification to Promote Cell Attachment to Hydrophobic Substrates. *J. Biomed. Mater. Res.* **1998**, *40*, 511−519.

(17) Mark Saltzman, W. Cell Interactions with Polymers. In *Principles of Tissue Engineering*, Second ed.; Robert, P. L., Robert, L., Joseph, V., Eds.; Academic Press: San Diego, CA, 2000; Chapter 19, pp 221−235.

(18) Hsin, I. C.; Yiwei, W., Cell Responses to Surface and Architecture of Tissue Engineering Scaffolds. In *Regenerative Medicine and Tissue Engineering - Cells and Biomaterials*, Eberli, D., Ed.; InTech: Winchester, U.K., 2011; Chapter 27.

(19) Aragon, J.; Gonzalez, R.; Fuentes, G.; Palin, L.; Croce, G.; Viterbo, D. Development and Characterization of a Novel Bioresorbable and Bioactive Biomaterial Based on Polyvinyl Acetate, Calcium Carbonate and Coralline Hydroxyapatite. *Mater. Res. (Sao Carlos, Braz.)* **2011**, *14*, 25−30.

(20) Demirbilek, M. E.; Demirbilek, M.; Karahaliloglu, Z.; Erdal, E.; Vural, T.; Yalcin, E.; Saglam, N.; Denkbas, E. B. Oxidative Stress Parameters of L929 Cells Cultured on Plasma-Modified Pdlla Scaffolds. *Appl. Biochem. Biotechnol.* **2011**, *164*, 780−792.

(21) Croll, T. I.; O'Connor, A. J.; Stevens, G. W.; Cooper-White, J. J. Controllable Surface Modification of Poly(Lactic-co-Glycolic Acid) (Plga) by Hydrolysis or Aminolysis I: Physical, Chemical, and Theoretical Aspects. *Biomacromolecules* **2004**, *5*, 463−473.

(22) Cai, K. Y.; Yao, K. D.; Cui, Y. L.; Yang, Z. M.; Li, X. Q.; Xie, H. Q.; Qing, T. W.; Gao, L. B. Influence of Different Surface Modification Treatments on Poly(D,L-Lactic Acid) with Silk Fibroin and Their Effects on the Culture of Osteoblast in Vitro. *Biomaterials* **2002**, *23*, 1603−1611.

(23) Gamboa-Martinez, T. C.; Gomez Ribelles, J. L.; Gallego Ferrer, G. Fibrin Coating on Poly (L-Lactide) Scaffolds for Tissue Engineering. *J. Bioact. Compat. Polym.* **2011**, *26*, 464−477.

(24) Dee, K. C.; Puleo, D. A.; Bizios, R. *An Introduction to Tissue-Biomaterial Interactions*. Wiley-Liss: Hoboken, NJ, 2002; pp 149−172.

(25) Park, G. E.; Pattison, M. A.; Park, K.; Webster, T. J. Accelerated Chondrocyte Functions on Naoh-Treated Plga Scaffolds. *Biomaterials* **2005**, *26*, 3075−3082.

(26) Ghasemi-Mobarakeh, L.; Prabhakaran, M. P.; Morshed, M.; Nasr-Esfahani, M. H.; Ramakrishna, S. Bio-Functionalized Pcl Nanofibrous Scaffolds for Nerve Tissue Engineering. *Mater. Sci. Eng., C* **2010**, *30*, 1129−1136.

(27) Zhang, H. N.; Migneco, F.; Lin, C. Y.; Hollister, S. J. Chemically-Conjugated Bone Morphogenetic Protein-2 on Three-Dimensional Polycaprolactone Scaffolds Stimulates Osteogenic Activity in Bone Marrow Stromal Cells. *Tissue Eng., Part A* **2010**, *16*, 3441−3448.

(28) Jao, Y. P.; Liu, Z. H.; Cui, F. Z.; Zhou, C. R. Effect of Hydrolysis Pretreatment on the Formation of Bone-Like Apatite on Poly(L-

Lactide) by Mineralization in Simulated Body Fluids. *J. Bioact. Compat. Polym.* **2007**, *22*, 492−507.
(29) Combellas, C.; Kanoufi, F.; Mazouzi, D.; Thiebault, A.; Bertrand, P.; Medard, N. Surface Modification of Halogenated Polymers. 4. Functionalisation of Poly(Tetrafluoroethylene) Surfaces by Diazonium Salts. *Polymer* **2003**, *44*, 19−24.
(30) Zeb, G.; Gaskell, P.; Le, X. T.; Xiao, X.; Szkopek, T.; Cerruti, M. Decoration of Graphitic Surfaces with Sn Nanoparticles through Surface Functionalization Using Diazonium Chemistry. *Langmuir* **2012**, *28*, 13042−13050.
(31) Zhang, X.; Tretjakov, A.; Hovestaedt, M.; Sun, G.; Syritski, V.; Reut, J.; Volkmer, R.; Hinrichs, K.; Rappich, J. Electrochemical Functionalization of Gold and Silicon Surfaces by a Maleimide Group as a Biosensor for Immunological Application. *Acta Biomater.* **2013**, *9*, 5838−5844.
(32) Griffete, N.; Li, H.; Lamouri, A.; Redeuilh, C.; Chen, K.; Dong, C. Z.; Nowak, S.; Ammar, S.; Mangeney, C. Magnetic Nanocrystals Coated by Molecularly Imprinted Polymers for the Recognition of Bisphenol A. *J. Mater. Chem.* **2012**, *22*, 1807−1811.
(33) Corgier, B. P.; Marquette, C. A.; Blum, L. J. Diazonium-Protein Adducts for Graphite Electrode Microarrays Modification: Direct and Addressed Electrochemical Immobilization. *J. Am. Chem. Soc.* **2005**, *127*, 18328−18332.
(34) Viel, P.; Le, X. T.; Huc, V.; Bar, J.; Benedetto, A.; Le Goff, A.; Filoramo, A.; Alamarguy, D.; Noel, S.; Baraton, L.; Palacin, S. Covalent Grafting onto Self-Adhesive Surfaces Based on Aryldiazonium Salt Seed Layers. *J. Mater. Chem.* **2008**, *18*, 5913−5920.
(35) Allongue, P.; Delamar, M.; Desbat, B.; Fagebaume, O.; Hitmi, R.; Pinson, J.; Saveant, J. M. Covalent Modification of Carbon Surfaces by Aryl Radicals Generated from the Electrochemical Reduction of Diazonium Salts. *J. Am. Chem. Soc.* **1997**, *119*, 201−207.
(36) Murphy, A. R.; John, P. S.; Kaplan, D. L. Modification of Silk Fibroin Using Diazonium Coupling Chemistry and the Effects on Hmsc Proliferation and Differentiation. *Biomaterials* **2008**, *29*, 2829−2838.
(37) Mahouche-Chergui, S.; Gam-Derouich, S.; Mangeney, C.; Chehimi, M. M. Aryl Diazonium Salts: A New Class of Coupling Agents for Bonding Polymers, Biomacromolecules and Nanoparticles to Surfaces. *Chem. Soc. Rev.* **2011**, *40*, 4143−4166.
(38) Shuttlew, A.; Veis, A. The Isolation of Anionic Phosphoproteins from Bovine Cortical Bone Via the Periodate Solubilization of Bone Collagen. *Biochim. Biophys. Acta* **1972**, *257*, 414−420.
(39) Spector, A. R.; Glimcher, M. J. The Extraction and Characterization of Soluble Anionic Phosphoproteins from Bone. *Biochim. Biophys. Acta* **1972**, *263*, 593−603.
(40) Murphy, W. L.; Mooney, D. J. Bioinspired Growth of Crystalline Carbonate Apatite on Biodegradable Polymer Substrata. *J. Am. Chem. Soc.* **2002**, *124*, 1910−1917.
(41) Liao, C. J.; Chen, C. F.; Chen, J. H.; Chiang, S. F.; Lin, Y. J.; Chang, K. Y. Fabrication of Porous Biodegradable Polymer Scaffolds Using a Solvent Merging/Particulate Leaching Method. *J. Biomed. Mater. Res.* **2002**, *59*, 676−681.
(42) Kokubo, T.; Takadama, H. How Useful Is SBF in Predicting in Vivo Bone Bioactivity? *Biomaterials* **2006**, *27*, 2907−2915.
(43) Pinson, J.; Podvorica, F. Attachment of Organic Layers to Conductive or Semiconductive Surfaces by Reduction of Diazonium Salts. *Chem. Soc. Rev.* **2005**, *34*, 429−439.
(44) Lyskawa, J.; Belanger, D. Direct Modification of a Gold Electrode with Aminophenyl Groups by Electrochemical Reduction of in Situ Generated Aminophenyl Monodiazonium Cations. *Chem. Mater.* **2006**, *18*, 4755−4763.
(45) Pinson, J. Attachment of Organic Layers to Materials Surfaces by Reduction of Diazonium Salts. In *Aryl Diazonium Salts*; Wiley-VCH Verlag GmbH & Co. KGaA: Weinheim, Germany, 2012; pp 1−35.
(46) Wildgoose, G. G.; Leventis, H. C.; Davies, I. J.; Crossley, A.; Lawrence, N. S.; Jiang, L.; Jones, T. G. J.; Compton, R. G. Graphite Powder Derivatised with Poly-L-Cysteine Using "Building-Block" Chemistry - a Novel Material for the Extraction of Heavy Metal Ions. *J. Mater. Chem.* **2005**, *15*, 2375−2382.
(47) Galli, C. Radical Reactions of Arenediazonium Ions: An Easy Entry into the Chemistry of the Aryl Radical. *Chem. Rev.* **1988**, *88*, 765−792.
(48) Laforgue, A.; Addou, T.; Belanger, D. Characterization of the Deposition of Organic Molecules at the Surface of Gold by the Electrochemical Reduction of Aryldiazonium Cations. *Langmuir* **2005**, *21*, 6855−6865.
(49) Doppelt, P.; Hallais, G.; Pinson, J.; Podvorica, F.; Verneyre, S. Surface Modification of Conducting Substrates. Existence of Azo Bonds in the Structure of Organic Layers Obtained from Diazonium Salts. *Chem. Mater.* **2007**, *19*, 4570−4575.
(50) Simionescu, C.; Popa, M. I.; Dumitriu, S. Bioactive Polymers XXX. Immobilization of Invertase on the Diazonium Salt of 4-Aminobenzoylcellulose. *Biotechnol. Bioeng.* **1987**, *29*, 361−365.
(51) Dolan, P. L.; Wu, Y.; Ista, L. K.; Metzenberg, R. L.; Nelson, M. A.; Lopez, G. P. Robust and Efficient Synthetic Method for Forming DNA Microarrays. *Nucleic Acids Res.* **2001**, *29*, E107−7.
(52) Ruffien, A.; Dequaire, M.; Brossier, P. Covalent Immobilization of Oligonucleotides on P-Aminophenyl-Modified Carbon Screen-Printed Electrodes for Viral DNA Sensing. *Chem. Commun.* **2003**, 912−913.
(53) Berthelot, T.; Garcia, A.; Le, X. T.; El Morsli, J.; Jegou, P.; Palacin, S.; Viel, P. "Versatile Toolset" for DNA or Protein Immobilization: Toward a Single-Step Chemistry. *Appl. Surf. Sci.* **2011**, *257*, 3538−3546.
(54) Zollinger, H. Formation and Reactions of Triazenes. In *Diazo Chemistry I*; Wiley-VCH Verlag GmbH & Co. KGaA: Weinheim, Germany, 2004; pp 385−404.
(55) Vaughan, K.; Stevens, M. F. G. Monoalkyltriazenes. *Chem. Soc. Rev.* **1978**, *7*, 377−397.
(56) Zollinger, H. Azo Coupling Reactions: Sections 12.1−12.6. In *Diazo Chemistry I*; Wiley-VCH Verlag GmbH & Co. KGaA: Weinheim, Germany, 2004; pp 305−346.
(57) Moulder, J. F.; Stickle, W. F.; Sobol, P. E.; Bomben, K. D. *Handbook of X-Ray Photoelectron Spectroscopy*; Perkin-Elmer Corp.: Eden Prarie, MN, 1992.
(58) Adenier, A.; Cabet-Deliry, E.; Chausse, A.; Griveau, S.; Mercier, F.; Pinson, J.; Vautrin-Ul, C. Grafting of Nitrophenyl Groups on Carbon and Metallic Surfaces without Electrochemical Induction. *Chem. Mater.* **2005**, *17*, 491−501.
(59) Le, X. T.; Viel, P.; Jegou, P.; Garcia, A.; Berthelot, T.; Bui, T. H.; Palacin, S. Diazonium-Induced Anchoring Process: An Application to Improve the Monovalent Selectivity of Cation Exchange Membranes. *J. Mater. Chem.* **2010**, *20*, 3750−3757.
(60) Gohier, A.; Nekelson, F.; Helezen, M.; Jegou, P.; Deniau, G.; Palacin, S.; Mayne-L'Hermite, M. Tunable Grafting of Functional Polymers onto Carbon Nanotubes Using Diazonium Chemistry in Aqueous Media. *J. Mater. Chem.* **2011**, *21*, 4615−4622.
(61) Gawalt, E. S.; Lu, G.; Bernasek, S. L.; Schwartz, J. Enhanced Bonding of Alkanephosphonic Acids to Oxidized Titanium Using Surface-Bound Alkoxyzirconium Complex Interfaces. *Langmuir* **1999**, *15*, 8929−8933.
(62) Viornery, C.; Chevolot, Y.; Leonard, D.; Aronsson, B. O.; Pechy, P.; Mathieu, H. J.; Descouts, P.; Gratzel, M. Surface Modification of Titanium with Phosphonic Acid to Improve Bone Bonding: Characterization by XPS and Tof-Sims. *Langmuir* **2002**, *18*, 2582−2589.
(63) Textor, M.; Ruiz, L.; Hofer, R.; Rossi, A.; Feldman, K.; Hahner, G.; Spencer, N. D. Structural Chemistry of Self-Assembled Monolayers of Octadecylphosphoric Acid on Tantalum Oxide Surfaces. *Langmuir* **2000**, *16*, 3257−3271.
(64) Jahromi, M. T.; Yao, G.; Cerruti, M. The Importance of Amino Acid Interactions in the Crystallization of Hydroxyapatite. *J. R. Soc., Interface* **2013**, *10*, 1742−5662.
(65) Gonçalves, C. M. B.; Coutinho, J. o. A. P.; Marrucho, I. M., Optical Properties. In *Poly(Lactic Acid)*; John Wiley & Sons, Inc.: New York, 2010; pp 97−112.

(66) Rehman, I.; Bonfield, W. Characterization of Hydroxyapatite and Carbonated Apatite by Photo Acoustic FTIR Spectroscopy. *J. Mater. Sci.: Mater. Med.* **1997**, *8*, 1−4.
(67) Kister, G.; Cassanas, G.; Vert, M.; Pauvert, B.; Terol, A. Vibrational Analysis of Poly(L-Lactic Acid). *J. Raman Spectrosc.* **1995**, *26*, 307−311.
(68) Auras, R.; Harte, B.; Selke, S. An Overview of Polylactides as Packaging Materials. *Macromol. Biosci.* **2004**, *4*, 835−864.
(69) Sopyan, I.; Mel, M.; Ramesh, S.; Khalid, K. A. Porous Hydroxyapatite for Artificial Bone Applications. *Sci. Technol. Adv. Mater.* **2007**, *8*, 116−123.
(70) Xie, Y. L.; Ding, H. S.; Qian, L. H.; Yan, X. M.; Yang, C. H.; Xie, Y. Y. Synthesis and Biological Evaluation of Novel Bisphosphonates with Dual Activities on Bone in Vitro. *Bioorg. Med. Chem. Lett.* **2005**, *15*, 3267−3270.